UNIABUJA Journal of Engineering and Technology

https://ujet.uniabuja.edu.ng/

ISSN: 2714-3236 (Online); 2714-3228 (Print)

Volume 3, Issue 2, 2026; 280-290

Vulnerability Assessment of Branch Failures in an Interconnected Power System Network

Isaiah A. ADEJUMOBI[1], Ayorinde J. OLANIPEKUN[2], Bakai I. OLAJUWON[3], Samuel A. OLAJIDE[4*]

[1,2]*Department of Electrical and Electronic Engineering, Federal University of Agriculture, Abeokuta, Ogun State, Nigeria*
[3]*Department of Mathematics, Federal University of Agriculture, Abeokuta, Ogun State, Nigeria*
[4]*Department of Electrical, Ogun-Oshun River Basin Development of Authority, Abeokuta, Ogun State, Nigeria*

[1]*adejumobia@funaab.edu.com,* [2]*olanipekunaj@funaab.edu.ng,* [3]*olajuwonbi@funaab.edu.ng,* [4*]*samueladeyemi500@gmail.com*

Abstract

Voltage instability has been a major concern to power supply utilities and its effect has resulted into system voltage collapse and high-power losses. This study employed fast voltage stability index technique (FVSI) to identify critical nodes and branches in an interconnected power system network, considering the IEEE 57-node electricity grids as case study. The modelling of the steady state characteristics of the network was carried out using load flow equations. The equations were linearized via Newton-Raphson iterative technique. Load flow modelling and simulation were carried out to determine the node voltage, phase angle and active power loss along the network lines. Simulations were done for the base case and the contingency-variation of the reactive loads in the network until FVSI value approaches one (1) to determine the maximum permissible load of each load nodes. The ranking in the system was done by sorting the maximum permissible load of the load nodes in ascending order. The smallest maximum permissible load was ranked highest implying that the node is the weakest in the system. The identified critical branches were corrected using static var compensator (SVC). Thereafter, the node voltage magnitudes and branch active power losses were computed and compared for the case networks. The results revealed that, for IEEE 57-node power system, 43 node voltages out of 57 node voltages were outside the statutory limit of ± 5%. The total active power loss was 65.303 MW. The inclusion of SVC in the system corrected the voltage limit violations on the critical nodes while the total active power loss reduced by 43.29% to 37.039 MW. These results are indications that FVSI when appropriately applied can aid the identification of critical nodes and branches in power system network while the SVC installation can minimise the power loss and improve the voltage magnitude of the system. This study established the suitability of fast voltage stability index technique for the weak nodes and branches identification in a power system for possible remedial action.

Keywords: *SVC, FVSI, Base Case, Contigency, Power Loss.*

1.0 Introduction

Modern power systems represent some of the most complex and advanced infrastructures developed by humanity, comprising a vast, interconnected network of components including generators, transformers, transmission lines, cables, and diverse loads designed to deliver reliable electricity to consumers across great distances (Dudek et al., 2023; Lopes et al., 2019). The increasing integration of renewable energy sources, rapid load growth, and evolving grid architectures have intensified the operational complexity and stress on these systems, often pushing transmission lines to their thermal and stability limits (Meegahapola et al.,2020; Mart'inez-Barbeito et al., 2023; Swain et al., 2022).This has led to widespread challenges such as transmission congestion, overloading, voltage instability, and, in severe cases, system-wide blackouts (Mart'inez-Barbeito etal., 2023; Adegoke and Sun, 2022; Simpson-Porco et al.,2016). A critical concern for power system engineers is maintaining voltage stability, which ensures that voltages remain within acceptable limits under both normal and disturbed conditions (Baleboina and Mageshvaran, 2023; Zeitawyeh and Faza, 2025; Werkie et al., 2025). Voltage instability is frequently triggered by insufficient reactive power support, high load demand, and the growing presence of power electronic converter-interfaced renewable generation, all of which can reduce system inertia and reactive power reserves (Meegahapola et al.,2020; Eladl et al., 2023; Anthony and Arunachalam, 2025; Sudame et al., 2024).

The consequences of voltage instability include cascading failures and large-scale outages, underscoring the need for continuous monitoring and advanced assessment techniques (Baleboina and Mageshvaran ,2023; Ratra et al., 2018; Park et al.,2021). Recent research emphasizes the importance of voltage stability indices, real-time monitoring, and optimal reactive power management including the deployment of flexible AC transmission system (FACTS) devices and distributed generation to enhance system resilience and prevent voltage collapse (Baleboina and Mageshvaran ,2023; Zeitawyeh and Faza, 2025; Sudame et al., 2024).

As power systems continue to evolve with increased renewable integration and bidirectional power flows, ensuring stable, dependable, and secure operation remains a central challenge for system planners and

Received: 31-03-2026 / Accepted: 25-04-2026 / Published: 27-06-2026

https://doi.org/10.70118/ujet.2026.0302.24

operators worldwide (Meegahapola et al., 2020; Anthony and Arunachalam, 2025; Lopes et al., 2019; Del Giudice et al., 2022). When voltage angle difference is minimal, the Fast Voltage Stability Index (FVSI) has the advantage of speed and precision; but, when angle difference is considerable, it is a sign of impending voltage collapse (Dora et al., 2025). In most literature reviewed, the power system with different loading condition were mostly considered without the compensation techniques. The gap was filled by considering the power system network under varying condition together with the compensation technique to rectify the voltage imbalance. Hence this paper presents accurate procedure of detecting critical lines and vulnerable load bus on power network for optimum placement of compensation devices (SVC).

2.0 Methodology

2.1 Fast Voltage Stability Index

The Fast Voltage Stability Index (FVSI) is calculated by applying the same voltage collapse point properties. Figure 1 displays a one-line illustration of a two-bus power system model. The variables and parameters are all in per unit**.**

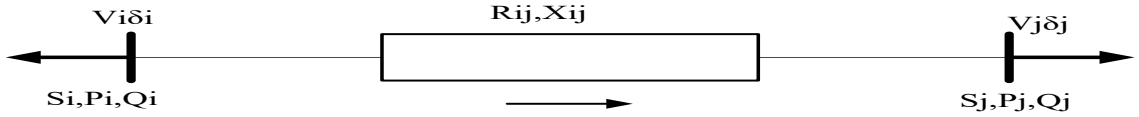

Figure 1: One-Line Diagram of a Two-Bus System Model (Bazilah et al., 2022)

Between buses I and J, R, X, Z and θ represent the line resistance, line reactance, line impedance and line impedance angle.
Real, reactive and apparent power at bus I are represented by Pi, Qi and Si respectively.
Real, reactive and apparent power at bus j are denoted by Pj, Qj and Sj respectively.
Vj and Vi are the voltage magnitudes at buses I and J, respectively.
At buses I and J respectively, δi and δj represent the voltage angle.
Real and reactive power measurements at the receiving end bus are the first step in the creation of all VSIs.

$$S_R = V_R I^* \tag{1}$$

Re-arranged (1)

$$I = \left(\frac{S_R}{V_R}\right)^* = \frac{\left(P_R - jQ_R\right)}{V_R \angle -\delta_R} \tag{2}$$

The current through line connected between two buses is expressed using Kirchoff voltage law (KVL)

$$I = \frac{V_S \angle \delta_S - V_R \angle \delta_R}{R + jX} \tag{3}$$

Substituting (2) into (3)

$$\frac{P_R - jQ_R}{V_R \angle -\delta_R} = \frac{V_S \angle \delta_S - V_R \angle \delta_R}{R + jX} \tag{4}$$

Cross multiply

Received: 31-03-2026 / Accepted: 25-04-2026 / Published: 27-06-2026

https://doi.org/10.70118/ujet.2026.0302.24

$$\left(R + jX\right)\left(P_R - jQ_R\right) = \left(V_R\angle -\delta_R\right)\left(V_S\angle\delta_S - V_R\angle\delta_R\right) \tag{5}$$

Expanding the L.H.S and R.H.S

$$P_R R - jRQ_R + jXP_P + XQ_R = \left(V_R V_S\angle\delta_S - \delta_R - V_R^2\angle -\delta_R + \delta_R\right) \tag{6}$$

$$P_R R - jRQ_R + jXP_P + XQ_R = \left(V_R V_S\angle\delta_S - \delta_R - V_R^2\angle 0\right) \tag{7}$$

Let $\delta_S - \delta_R = \delta$ and equation (7) can be simplified as

$$P_R R + jXP_R + XQ_R - jRQ_R = \left(V_R V_S\angle\delta - V_R^2\right) \tag{8}$$

By Changing $V_R V_S\angle\delta$ from polar form into rectangular form

$$P_R R + jP_R X + Q_R X - jQ_R R = V_R V_S\,\mathrm{Cos}\,\delta + jV_R V_S\,\mathrm{Sin}\,\delta - V_R^2 \tag{9}$$

By separating the equation (9) into real part and imaginary part,

$$P_R R + Q_R X + j\left(P_P X - Q_R R\right) = V_R V_S\,\mathrm{Cos}\,\delta + jV_R V_S\,\mathrm{Sin}\,\delta - V_R^2 \tag{10}$$

The real part

$$P_R R + Q_R X = V_R V_S\,\mathrm{Cos}\,\delta - V_R^2 \tag{11}$$

The Imaginary part

$$P_R X - Q_R R = V_R V_S\,\mathrm{Sin}\,\delta \tag{12}$$

Re-arrange equation (11)

$$P_R R = V_R V_S\,\mathrm{Cos}\,\delta - V_R^2 - Q_R X \tag{13}$$

$$P_R = \frac{V_R V_S\,\mathrm{Cos}\,\delta - V_R^2 - Q_R X}{R} \tag{14}$$

Re-arrange equation (14)

$$P_R X - Q_R R = V_R V_S\,\mathrm{Sin}\,\delta \tag{15}$$

$$Q_R = \frac{P_R X - V_R V_S\,\mathrm{Sin}\,\delta}{R} \tag{16}$$

Substituting equation (16) into equation (14) and equation (14) into equation (16)

$$P_R = \frac{V_R V_S\,\mathrm{Cos}\,\delta - V_R^2 - X\left(\dfrac{P_R X - V_R V_S\,\mathrm{Sin}\,\delta}{R}\right)}{R} \tag{17}$$

Received: 31-03-2026 / Accepted: 25-04-2026 / Published: 27-06-2026
https://doi.org/10.70118/ujet.2026.0302.24

$$Q_R = \frac{\left(\frac{V_R V_S \cos\delta - V_R^2 - Q_R X}{R}\right) X - V_R V_S \operatorname{Sin}\delta}{R} \tag{18}$$

Re-arranging equation (17) and (18)

$$V_R^2 - V_S V_R \left(\cos\delta + \frac{X \sin\delta}{R}\right) + P_R \left(R + \frac{X^2}{R}\right) = 0 \tag{19}$$

$$V_R^2 + V_S V_R \left(\frac{R \sin\delta}{X} - \cos\delta\right) + Q_R \left(X + \frac{R^2}{X}\right) = 0 \tag{20}$$

By clearing the fraction and rearranged the equation (20) as follows

$$XV_R^2 + V_S V_R \left(R \sin\delta - X \cos\delta\right) + Q_R \left(X^2 + R^2\right) = 0 \tag{21}$$

The roots of the above quadratic are obtained as

$$V_R = \frac{V_S (X \cos\delta - R \sin\delta \pm \sqrt{\left(V_S \left(R \sin\delta - X \cos\delta\right)\right)^2 - 4X\left(Q_R \left(X^2 + R^2\right)\right)}}{2X} \tag{22}$$

The real and nonzero value of VR can be determined by setting a discriminant of greater than zero

$$\left(V_S \left(R \sin\delta - X \cos\delta\right)\right)^2 - 4X\left(Q_R \left(X^2 + R^2\right)\right) \geq 0 \tag{23}$$

$$R^2 + X^2 = Z^2 \tag{24}$$

$$\left(V_S \left(R \sin\delta - X \cos\delta\right)\right)^2 - 4X\left(Q_R \left(Z^2\right)\right) \geq 0 \tag{25}$$

Hence, the new index

$$FVSI = \frac{4XQ_R Z^2}{\left(V_S \left(R \sin\delta - X \cos\delta\right)\right)^2} \leq 1 \tag{26}$$

Considering that the angle difference δ is negligible, that is, if δ is zero, then sinδ is zero and cosδ is one. Therefore,

$$FVSI = \frac{4Q_R Z^2}{XV_S^2} \leq 1 \tag{27}$$

The FVSI value which is between 0 and 1 must be less than unity in order to maintain the stability of the system's voltage. Lines with an FVSI greater than unity indicate buses where lines are connected and are undergoing a sudden voltage drop that is approaching system failure.

The IEEE 57-bus test system was used to validate the FVSI in the study. Here, the findings are examined.

2.2 An explanation of the case study

This study uses the IEEE 57-bus power system network shown in figure 2 as case study.

Received: 31-03-2026 / Accepted: 25-04-2026 / Published: 27-06-2026

https://doi.org/10.70118/ujet.2026.0302.24

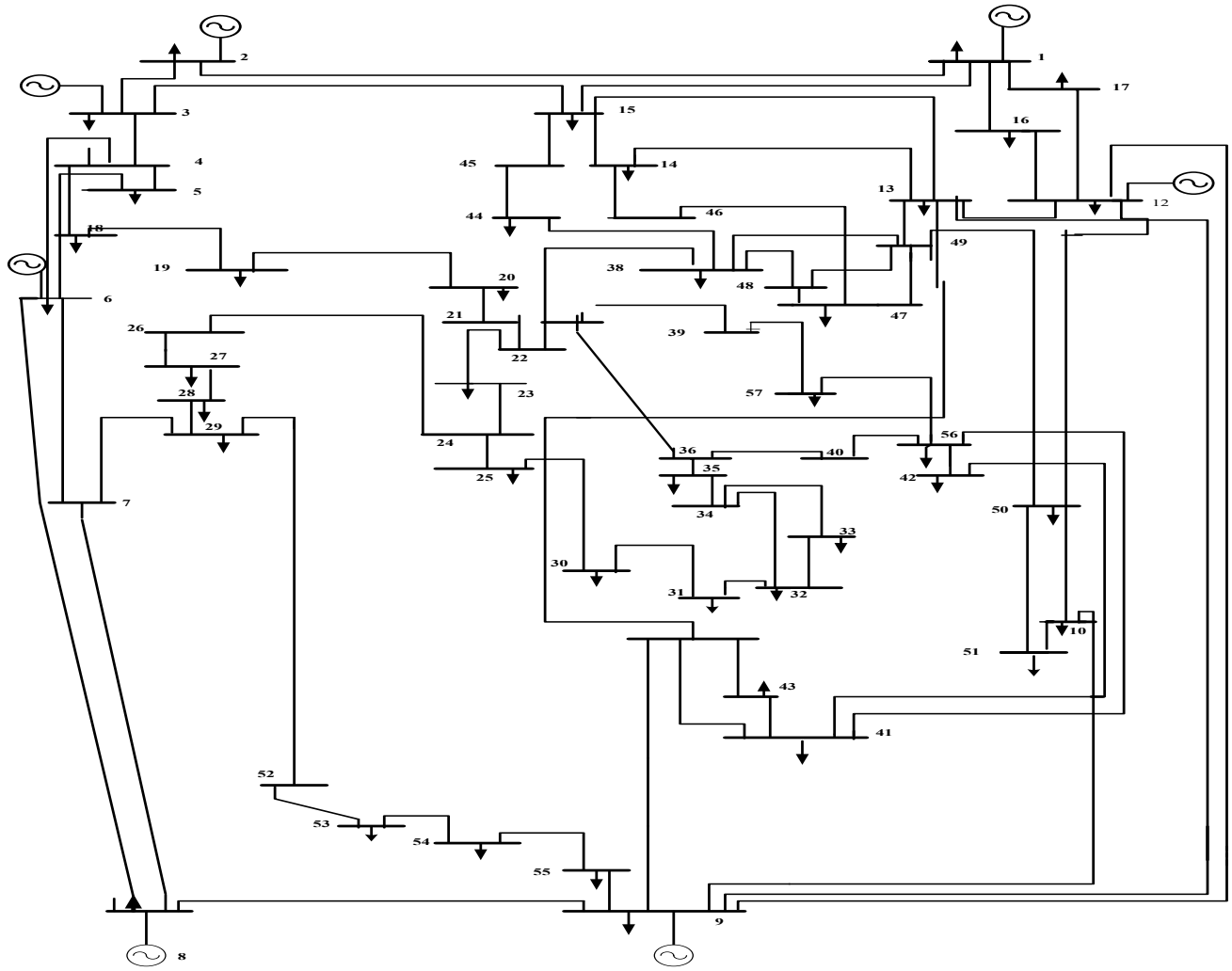

Figure 2: Single line diagram of the IEEE 57-Bus System

Load flow modelling and simulation were carried out to determine the node voltage, phase angle and active power loss along the network lines. The FVSI used to identify essential nodes and transmission lines in an interconnected power network, was also simulated. All the simulations were carried out in MATLAB 2018b environment. The findings of the simulations, on the IEEE 57-Bus power systems networks were obtained.

2.3 Simulations

Two scenarios were considered in the simulations. These are:

i. the base case – representing the normal operating mode

ii. the contingency case – representing the unforeseen variations in the reactive power of the load buses from the base case one per time. The maximum reactive load for each load bus on the IEEE 57-Bus power system was determined to identify the weak bus and critical line of the bus, the reactive loads on the load buses were changed one at a time.

Static Var Compensator (SVC) was applied to improve the voltage profile at the buses and minimize the active power loss on the transmission lines; the Fast Voltage Stability Index was determined to identify the essential transmission lines and susceptible buses. The voltage magnitude and line flows were simulated and compared before and after compensation. The flow chart of the simulation is shown in figure 3

Received: 31-03-2026 / Accepted: 25-04-2026 / Published: 27-06-2026

https://doi.org/10.70118/ujet.2026.0302.24

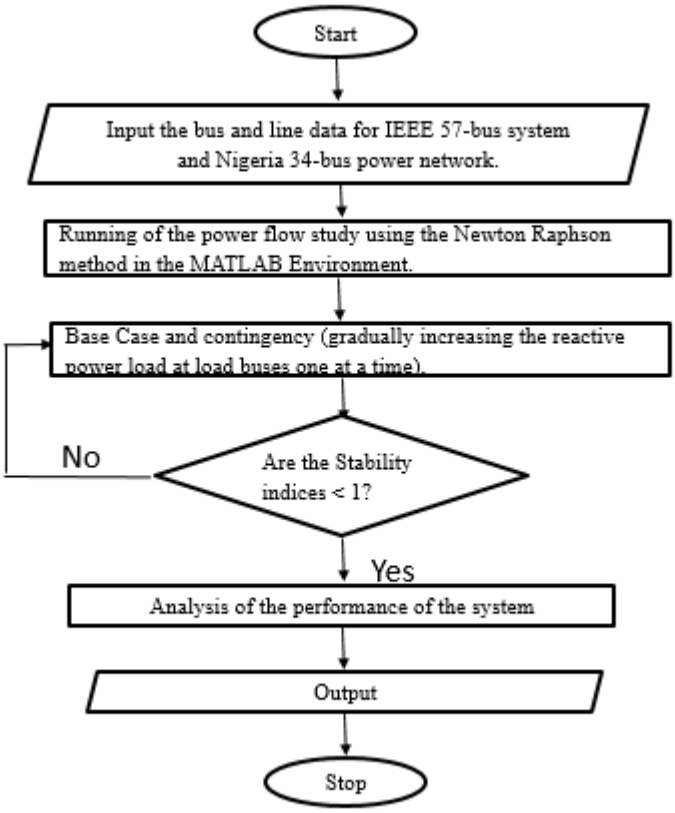

Figure 3: Flow chart for calculating the voltage stability indices

3.0 Results and Discussion

3.1 Base case results

These include the results for the voltage magnitude profile and FVSI values of the IEEE 57-Bus Power System for Base Case. Figure 3 shows the chart of voltage profile for the IEEE 57-Bus system and Figure 4 shows the chart of FVSI against Line number.

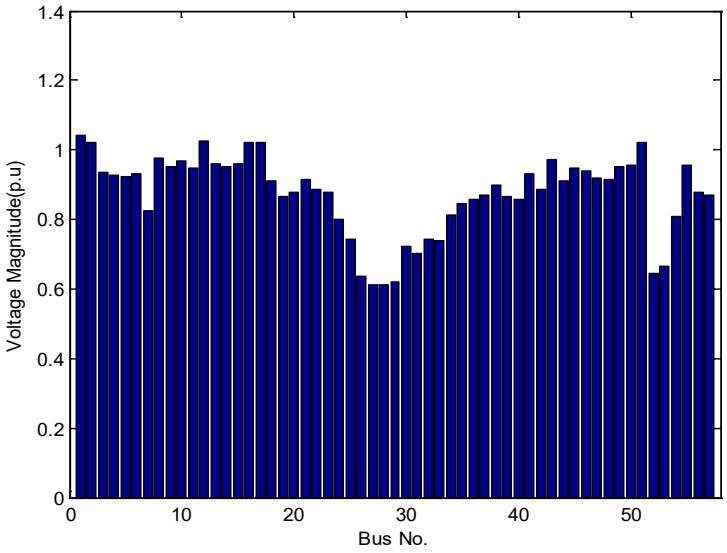

Figure 4: The bar chart of voltage profile for the IEEE 57-Bus Power System

Received: 31-03-2026 / Accepted: 25-04-2026 / Published: 27-06-2026
https://doi.org/10.70118/ujet.2026.0302.24

In figure 4, the results revealed that, for IEEE 57-node power system, 43 node voltages out of 57 node voltages were outside the statutory limit of ± 5%.

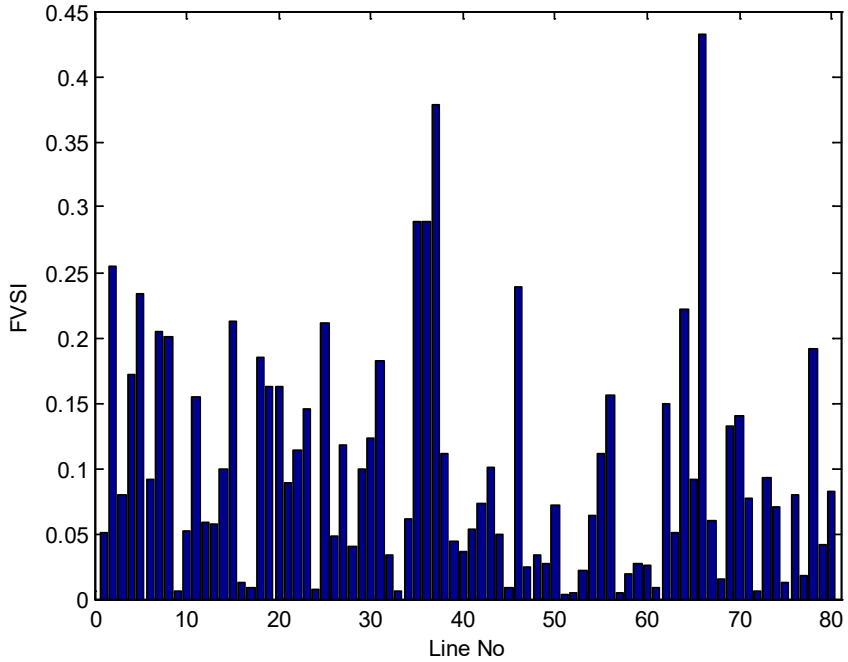

Figure 5: The bar chart of FVSI against Line Number for the base case

In Figure 5, all the Fast Voltage Stability Index values of the Line Numbers are far below 1. Since all of the indices are less than one (< 1), simulation results for the IEEE 57-bus test for the base case demonstrate that the system is stable.

3.2 Contingency Analysis Result

Table 1 shows the simulation results for determining the maximum reactive load for each load bus on the IEEE 57-Bus power system.

Table1: contingency Analysis: Maximum Loadability and Ranking for IEEE 57-Bus Test System

S/N	Bus No	From bus	To bus	Vmag (pu)	Qmax (MVAr)	FVSI	Ranking
1	32	34	32	0.8036	12	0.9205	1
2	33	34	32	0.8025	13	0.9323	2
3	31	31	32	0.5475	14	0.864	3
4	30	24	25	0.8067	16	1.0035	4
5	25	24	25	0.8205	18	0.9438	5
6	20	21	20	0.8997	25	0.9596	6
7	19	18	19	0.8758	28	0.9947	7
8	57	39	57	0.8521	29	0.9439	8
9	24	26	27	0.7485	31	0.9762	9
10	56	56	41	0.7067	36	0.9672	10
11	26	26	27	0.7152	39	0.9606	11
12	42	41	42	0.7951	41	0.9932	12
13	34	24	26	0.7614	46	0.8632	13
14	41	41	43	0.7202	55	0.97856	14
15	54	54	55	0.8131	57	0.9789	15
16	40	40	56	0.5768	64	0.9718	16
17	35	24	26	0.7298	63	1.0132	17

Received: 31-03-2026 / Accepted: 25-04-2026 / Published: 27-06-2026

https://doi.org/10.70118/ujet.2026.0302.24

S/N	Bus No	From bus	To bus	Vmag (pu)	Qmax (MVAr)	FVSI	Ranking
18	21	21	22	0.6803	71	0.9757	18
19	36	37	38	0.6571	72	1.0002	19
20	18	4	18	0.9172	72	1.0727	20
21	39	37	38	0.6602	73	1.0014	21
22	53	53	54	0.7036	73	0.9894	22
23	52	29	52	0.9073	74	0.9975	23
24	37	37	38	0.6631	78	1.0042	24
25	27	27	28	0.6498	82	0.9739	25
26	23	24	26	0.7388	84	0.9933	26
27	22	24	26	0.7378	91	0.9952	27
28	50	50	51	0.776	100	0.9919	28
29	43	11	43	0.8879	109	0.9747	29
30	38	24	26	0.7331	125	1.0109	30
31	28	28	29	0.6660	127	0.9942	31
32	49	13	49	0.9360	128	0.9880	32
33	44	24	26	0.7331	132	1.0012	33
34	48	24	26	0.7328	139	1.0004	34
35	55	9	55	0.9400	154	0.9975	35
36	47	24	26	0.7302	161	1.0012	36
37	51	10	12	0.776	180	1.0000	37
38	45	15	45	0.90119	186	0.9884	38
39	10	10	12	0.7735	198	1.0058	39
40	29	7	29	0.8264	200	0.9994	40
41	46	24	26	0.7307	205	0.9929	41
42	5	5	6	0.7697	259	1.0003	42
43	17	1	17	1.0400	263	1.0006	43
44	16	1	16	1.0400	278	1.0015	44
45	11	9	11	0.9300	325	0.9892	45
46	7	7	8	0.7606	327	0.9993	46
47	14	24	26	0.7227	407	1.0019	47
48	4	4	6	0.7615	490	1.0011	48
49	15	1	15	1.0400	605	0.9991	49
50	13	12	13	1.0400	610	0.9999	50

Table 1 displays each bus's maximum loadability, or its maximum reactive load capacity, as well as the bus ranking according to load. The line is designated as the most susceptible and crucial line, and the load bus with the lowest maximum load capacity is designated as the weakest bus according to Table.1's rankings. Bus 32, the weakest bus, ranks first and has the lowest maximum load capacity. Bus 32 was identified as the weakest bus in the contingency scenario since its index values were quite near to one (~ 1). This indicates that voltage collapse is imminent, that line 32-34 is the crucial line, and that the maximum allowable reactive loading is 12 MVA. Accordingly, bus 12 is the best spot to install a potential compensating device to enhance the bus's voltage profile and prevent voltage collapse. The critical voltage for bus 32 is 0.8036, which is the voltage at which the bus is operating at its maximum allowable load.

The maximum loadability, or its maximum reactive load capacity were displayed, as well as the bus ranking according to load. The line is designated as the most susceptible and crucial line, and the load bus with the lowest maximum load capacity is designated as the weakest bus according to the rankings. Bus 32, the weakest bus, ranks first and has the lowest maximum load capacity.

Received: 31-03-2026 / Accepted: 25-04-2026 / Published: 27-06-2026

https://doi.org/10.70118/ujet.2026.0302.24

3.3. Voltage profile of the IEEE 57-bus power system before and compensation with SVC

The comparison of the voltage profile of the IEEE 57 - bus power system with and without compensation is shown in figure 6.

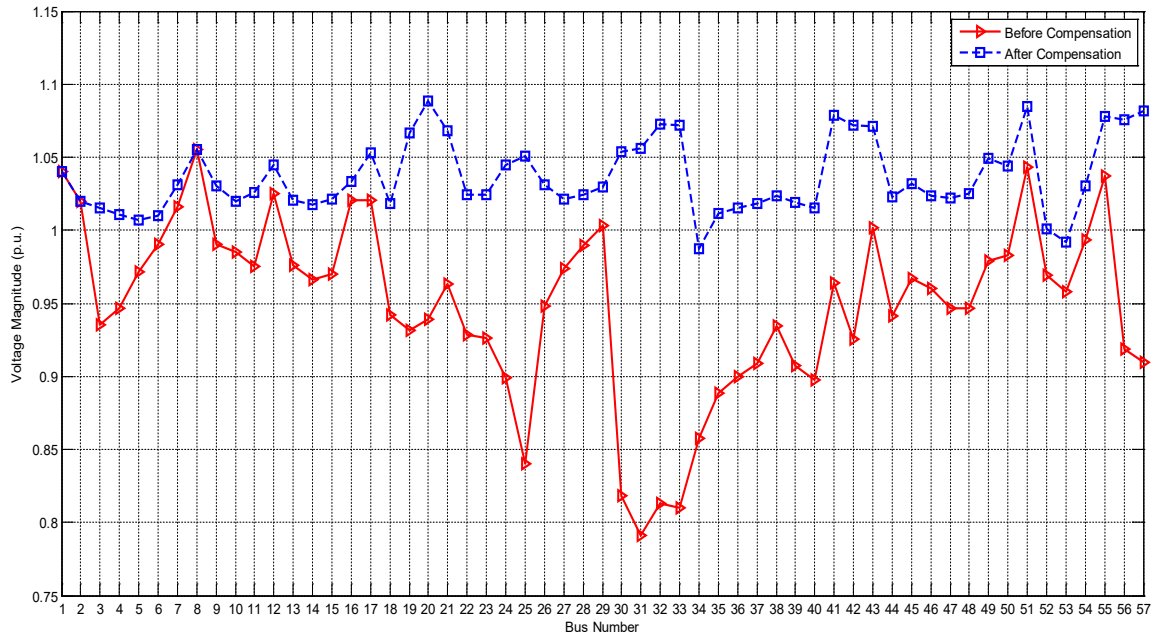

Figure 6: Comparison of the Voltage profile of the IEEE 57 - Bus Power system with and without compensation

From the figure 6, it could be observed that the voltage profile of the overall network improved with compensation compared to when no SVC was applied. The voltage magnitude of the buses below the acceptable limit (0.95) from the initial load flow analysis which was validated by the Fast Voltage Stability Index (FVSI) computations had increased drastically. This result shows that SVC had a positive impact on the overall network performance. The obtained system's voltage profile with and without SVC compensation are presented in graph for easy view comparison.

3.4 Power Losses minimization of the IEEE57-Bus Power Network before and after compensation.

Received: 31-03-2026 / Accepted: 25-04-2026 / Published: 27-06-2026
https://doi.org/10.70118/ujet.2026.0302.24

Figure 7 shows the comparison of the line flow of IEEE 57- Bus Power system before and after compensation.

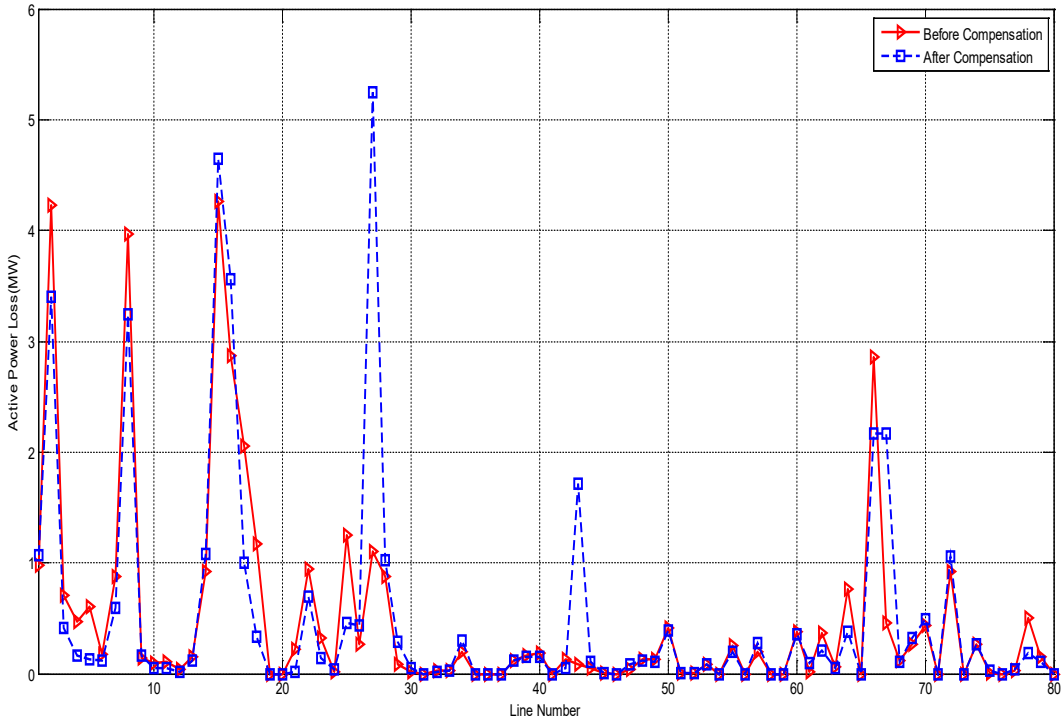

Figure 7: Comparison of the line flow of IEEE 57- Bus Power system before and after compensation

From Figure 7, the total active loss of the system was 65.303 MW without compensation reduced to 37.039 MW with the inclusion of SVC; therefore, producing an improvement of 43.29% in the system' total active power loss. This result shows that SVC had positive impact on over all network performance. The obtained active power loss with and without SVC compensation are presented in graph for easy view comparison.

4.0 Conclusion

In this research work, the power flow results using Newton Raphson (NR) iterative technique were generated on the IEEE 57-bus test system. The voltage magnitude at the buses and power loss on the transmission lines were calculated from the power flow solutions. With the employment of a Static Var Compensator (SVC) to enhance the voltage profile at the buses and reduce the active power loss on the transmission lines, the Fast Voltage Stability Index was calculated to identify the essential transmission lines and susceptible buses. Consequently, when a power system network experiences a voltage stability issue, the system was redesigned to improve the network's voltage profile and stabilize the power system network.

References

Adegoke, S., & Sun, Y., (2022). Power system optimization approach to mitigate voltage instability issues: A review. Cogent Engineering. 2025(1) 1-40.

Anthony, K., & Arunachalam, V., (2025). Voltage Stability Monitoring and Improvement in a Renewable Energy Dominated Deregulated Power System: A Review. e-Prime - Advances in Electrical Engineering, Electronics and Energy 11,1-12.

Bakkabulindi, G., Ndayishimiye, V., & Miyingo, E., (2025). Optimal Grid Expansion Planning in Power Systems with Surplus Generation Capacity and Suppressed Demand. The Journal of Engineering 2025 (1), 1-11.

Baleboina, G., & Mageshvaran, R. (2023). A survey on voltage stability indices for power system transmission and distribution. Frontiers in Energy Research, 11:1159410.

Del Giudice, D., Bizzarri, F., Grillo, S., Linaro, D., & Brambilla, A., (2022). Impact of Passive-Components' Models on the Stability Assessment of Inverter-Dominated Power Grids. Energies 2022 15(17), 6348.

Dobson, I., Parashar, M., & Carter, C. (2010). Combining phasor measurements to monitor cutset angles. In system Sciences (HICSS), 2010 43rd Hawaii International conference on (pp.1-9). IEEE.

Dora, B., Bhat, S., Mitra, A., Ernst, D., Halinka, A., Zychma, D., & Sowa, P., (2025). The Global Electricity Grid: A Comprehensive Review. Energies 2025 18 (5), 1152.

Dudek, G., Piotrowski, P., & Baczyński, D., (2023). Intelligent Forecasting and Optimization in Electrical

Received: 31-03-2026 / Accepted: 25-04-2026 / Published: 27-06-2026

https://doi.org/10.70118/ujet.2026.0302.24

Power Systems: Advances in Models and Applications. Energies 2023, 16(7), 3024.
Eladl, A., Basha, M., & Eldesouky, A., (2023). Techno-economic multi-objective reactive power planning in integrated wind power system with improving voltage stability. Electric Power Systems Research, 214(A),108917.
Fernandes, R., Lirio, F., De Oliveira, B., & De Lima, A., (2025). Performance Comparison of LCC and VSC HVDC Systems in Minimizing Long-Term Voltage Collapse. IEEE Access, 13, 53965-53979.
Ismail, B., Mohammad, L.O., Noor I.A.W., Mohd, A.M.R; Kanendra; N.V; Muhammad, N.M.N., and Mohd, K.R., (2022). New Line Voltage Stability Index (BVSI) for voltage stability Assessment in power system.10, 103906-10393.
Lopes, J., Madureira, A., Matos, M., Bessa, R., Monteiro, V., Afonso, J., Santos, S., Catalão, J., Antunes, C., & Magalhães, P., (2019). The future of power systems: Challenges, trends and upcoming paradigms. Wiley Interdisciplinary Reviews: Energy and Environment 9 (3) e368.
Mart'inez-Barbeito, M., Gomila, D., Colet, P., Fritzsch, J., & Jacquod, P., (2023). Transmission grid stability with large interregional power flows. Physical Review Research. 7 (1), 013137.
Meegahapola, L., Sguarezi, A., Bryant, J., Gu, M., Conde, R., & Cunha, R., (2020). Power System Stability with Power-Electronic Converter Interfaced Renewable Power Generation: Present Issues and Future Trends. Energies 2020, 13(13), 3441.
Panda, M., & Nayak, Y., (2022). Impact analysis of renewable energy Distributed Generation in deregulated electricity markets: A context of Transmission Congestion Problem. Energy. 254, (C), 124403.
Park, B., Im, S., Kim, D., & Lee, B., (2021). Clustered Effective Reactive Reserve to Secure Dynamic Voltage Stability in Power System Operation. IEEE Transactions on Power Systems 36, 1183-1192.
Ratra, S., Tiwari, R., & Niazi, K., (2018). Voltage stability assessment in power systems using line voltage stability index.Comput.Electr.Eng.,70,199211.
Simpson-Porco, J., Dörfler, F., & Bullo, F., (2016). Voltage collapse in complex power grids. Nature Communications2016, 7(1), 10790.
Sudame, B., Patil, G., Kasar, A., Babar, S., Pawar, P., & Yewale, S., (2024). Enhancing Voltage Stability Through Optimal Reactive Power Management in Power Systems. Nanotechnology Perceptions.
Swain, A., Abdellatif, E., Mousa, A., & Pong, P., (2022). Sensor Technologies for Transmission and Distribution Systems: A Review of the Latest Developments. Energies 2022, 15(19), 7339.
Werkie, Y., Nyakoe, G., & Wekesa, C., (2025). Power System Voltage Stability Assessment and Control Strategies: State-of-the-Art Review. J. Electr. Comput. Eng., 2025(1) 1-24.
Zeitawyeh, R., & Faza, A., (2025). Optimal Reactive Power Planning Using FACTS Devices for Voltage Stability Enhancement in Power Transmission Systems. Energy Science & Engineering, 13 (6). 2720-2756.

Received: 31-03-2026 / Accepted: 25-04-2026 / Published: 27-06-2026

https://doi.org/10.70118/ujet.2026.0302.24